04

# Four-wave mixing by phase-amplitude holographic gratings in the photorefractive piezocrystal of $\bar{4}3m$ symmetry class

© V.N. Naunyka

I.P. Shamyakin Mozyr State Pedagogical University, 247760 Mozyr, Gomel Region, Republic of Belarus

e-mail: valnav@inbox.ru

*Received November 16, 2021*
*Revised November 16, 2021*
*Accepted December 18, 2021*

A system of coupled-wave equations for calculating the vector amplitudes of linearly polarized light waves at four-wave mixing by phase-amplitude holographic gratings in a cubic photorefractive semiconductor of an arbitrary cut belonging to the $\bar{4}3m$ symmetry class is presented. The dependencies of the intensities of the polarization components of the reversed light wave on the orientation angle for GaAs crystal of (110)-cut are calculated on the basis of the numerical solution of the system of coupled wave equations. The obtained dependences are compared with the known theoretical and experimental data. It is shown that the best agreement between the results of theoretical modeling and experimental data at calculating the contra-directional four-wave mixing in GaAs crystal of (110)-cut is achieved if formation of several phase-amplitude holographic gratings is allowed, and the contribution of the photoelastic and inverse piezoelectric effects are taken into account together with absorption of the crystal.

**Keywords:** four-wave mixing, photorefractive semiconductor, light wave, holographic grating, coupled wave equations.

DOI: 10.21883/EOS.2022.03.53557.2936-21

## Introduction

Photorefractive crystals may be used as light-sensitive materials in devices designed for generation, processing and transmission of optical signals [1]. Due to the stationary amplification of the incident light beam and the possibility of creating a feedback providing wavefront reversal, photorefractive crystals are used in the design of dynamic grating lasers [2]. Cubic photorefractive semiconductors have a number of advantages over other photosensitive materials because of their relatively short photorefractive response time, low generation threshold by pumping wave capacity, and the ability to move into the infrared range of the spectrum [3].

The results of pioneering studies of wavefront reversal during four-wave mixing in photorefractive semiconductors are reported in papers [4–7]. The results of experimental observation of degenerate four-wave mixing in GaAs:EL2 crystal are given in [4]. The paper experimentally determines the photorefractive response time and predicts the possibility of using GaAs crystals in optical devices that must exhibit high speed and sensitivity. Practically simultaneously paper [5] is published, which provides the results of the experimental study of the regularities in the four-wave interaction in InP:Fe crystal. This paper studied the effect of an alternating electric field applied to the crystal on the intensity of the reversed light wave and mentions the possibility of using such crystals for processing optical signals in the infrared range. In the paper [6] studied the effect of an applied alternating electric field on the reflection coefficient in the four-wave mixing in a GaAs crystal, as well as the characteristics of the reversed wavefront. The largest experimentally measured stationary reflection coefficient for a GaAs crystal was 15%, with observed short-term increase in reflection coefficient up to 510%. In paper [7] demonstrated that recording of moving holographic gratings and applying a constant external electric field to a GaAs:Cr crystal causes the reflection coefficient to reach 500%.

Along with studies of wavefront reversal patterns in photorefractive semiconductors, the possibility of using such crystals in image processing devices and in optical oscillators is being investigated [8,9]. The results of experiments on wavefront reversal and image processing are presented in [8]. It is shown that GaAs crystals, despite their relatively small electro-optical coefficient, may be effectively used as recording media in image processing devices. The regularities of the four-wave mixing in Ga/AlGaAs semiconductor lasers were analyzed in [9]. The obtained results demonstrate that Ga/AlGaAs crystals can be an effective source of nonlinear optical interaction in lasers. Four-wave interaction is currently used to study and improve semiconductor quantum dot lasers (see, e.g., [10–12]).

Theoretical analysis of light waves diffraction on holographic gratings in cubic photorefractive crystals is quite complicated, since in addition to the linear electro-optical effect it requires additional consideration of some recording medium properties. When recording and reconstructing a holographic grating in a photorefractive piezocrystal, an essential role is played by elastic deformations arising from the induction of electric fields [13]. Presence of elastic deformations necessitates additional consideration of the photoelastic and inverse piezoelectric effects when calculating the modulation of the crystal dielectric permittivity at

optical frequencies. Anisotropy of the holographic grating in a cubic crystal with simultaneous consideration of linear electro-optical, photoelastic, and inverse piezoelectric effects is calculated in[14]. When calculating diffraction efficiency on a volume hologram, it is also necessary to take into account the fact that a holographic grating may have a phase-amplitude structure (mixed hologram) and represent a combination of phase and amplitude gratings [15,16]. A phase grating arises from the spatial modulation of the recording medium refraction index, and the amplitude grating — the absorption index. Contribution of the amplitude component may have a significant influence on the diffraction efficiency of a holographic grating formed in a cubic photorefractive crystal [17]. The paper shows that the best agreement between the theoretical and experimental data obtained in finding the orientation dependence of the diffraction efficiency of the transmission hologram formed in the $Bi_{12}TO_{20}$ (BTO) crystal is achieved by taking into account the phase/amplitude structure of the holographic grating. The experimental method for the separate study of the phase and amplitude holographic grating properties in GaAs and InP crystals, which is based on the study of diffracted beam intensity variation dynamics in four-wave mixing, is described in [18]. It is shown that the initial rapid decrease of the diffracted light beam intensity is caused by the erasure of the amplitude holographic grating and the subsequent smooth decrease in the intensity is caused by the erasure of the phase holographic grating.

In early theoretical papers the calculation of the four-wave mixing in cubic photorefractive crystals neglected the joint contribution of the photoelastic and inverse piezoelectric effects, the phase-amplitude structure of holograms and absorption, which could lead to noticeable deviations of theoretical data from experimental results [19]. Optimal conditions for wavefront reversal in cubic photorefractive crystals of 23 symmetry class taking into account photoelastic and inverse piezoelectric effects, optical activity, and absorption were calculated in [20]. Based on the solution of coupled wave equations, analytical expressions were found in the paper for the transmission and reflection coefficients in the four-wave mixing on a transmission holographic grating with a wave vector oriented in the crystallographic direction $[\bar{1}10]$, and the light waves whose wave normals lie in the plane (001). The threshold conditions are calculated for the generation of a reversed light front during the interaction of non-orthogonally polarized pumping light beams when an external meander electric field is applied to the crystal. Analysis of the regularities in the vector four-wave mixing on a reflection holographic grating in a cubic optically active photorefractive piezocrystal is performed in [21]. It is theoretically predicted in the paper that the reflection coefficient for a BTO : Fe, Cu crystal of thickness more than 3 mm may exceed 100% when orientations are optimally chosen by the vector of polarization of signal and pumping waves. A system of coupled wave equations suitable for calculating the reversed wave front at diffraction of light beams on a reflection holographic grating in a cubic photorefractive crystal of 23 symmetry class of arbitrary cut is presented. Features of four-wave mixing on phase-amplitude transmission gratings in a BTO crystal of (110)-cut with regard to photoelastic and inverse piezoelectric effects, optical activity, absorption, and circular dichroism have been studied in [22]. Dependence of the reversed light wave intensity on the orientation angle and crystal thickness was studied theoretically. It was found experimentally that in a 7.7 mm thick BTO crystal the reflection coefficient can reach 240%. The paper determines values of orientation angles corresponding to the highest values of the reflection coefficient. It is shown that the best agreement between theoretical and experimental data is achieved if the phase-amplitude structure of the transmission holographic gratings formed in the BTO crystal is taken into account.

As far as we know, the problem of analyzing the regularities of wavefront reversal on the phase-amplitude holographic gratings in cubic photorefractive crystals of symmetry class $\bar{4}3m$ with account of photoelastic and inverse piezoelectric effects has not been considered so far. When solving this problem it should be taken into account that in the general case of contra-directional four-wave mixing in a cubic photorefractive crystal, 6 phase-amplitude holographic gratings [2] can be formed simultaneously. Taking these features into account in the theoretical model will make it possible to find new regularities in the formation of the reversed wave front in four-wave mixing in a photorefractive semiconductor, to calculate the reflection and transmission coefficients more accurately, and to predict the optimal conditions for the generation of a phase-conjugated light wave.

The purpose of this study was to construct a mathematical model suitable for describing the degenerate contra-directional four-wave mixing on the phase-amplitude holographic gratings formed in a cubic photorefractive crystal of symmetry class $\bar{4}3m$, and to compare the theoretical data obtained on the basis of this model with the results of known experimental studies. When the mathematical model was developed, a case was considered, where a four-wave mixing in a photorefractive crystal generated 6 phase-amplitude holographic gratings, and the interacting waves have linear polarization. The theoretical model will also take into account linear electro-optical, photoelastic, and inverse piezoelectric effects, as well as the absorption of the crystal.

## Mathematical model

Let two pumping waves 1 and 2 and a signal wave 3 fall on a cubic photorefractive semiconductor (fig. 1). Let us assume that light waves are monochromatic linearly polarized and propagate in the incidence plane (I). Pumping waves 1 and 2 propagate in the directions indicated by unit vectors $\mathbf{e}_{1n}$ and $\mathbf{e}_{2n}$. Direction of signal wave propagation coincides in direction with the unit vector $\mathbf{e}_{3n}$. Wave 4 arises as a result of diffraction processes of pumping and

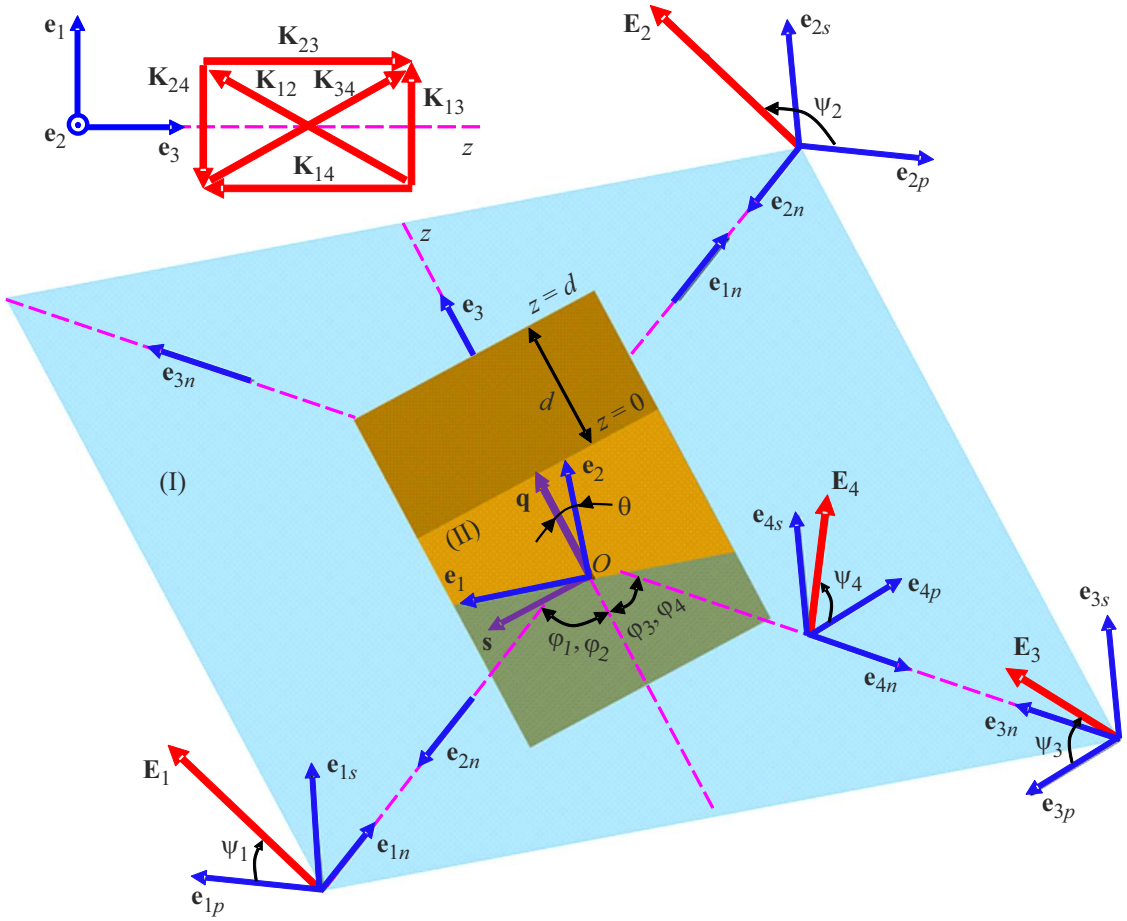


**Figure 1.** Scheme of contra-directional four-wave mixing in a photorefractive semiconductor.

signal waves on holographic gratings formed in the crystal and propagates in the direction of the unit vector $\mathbf{e}_{4n}$.

To describe the polarization state of $j$-th wave, we use orthonormalized basis $(\mathbf{e}_{jp}, \mathbf{e}_{js}, \mathbf{e}_{jn})$, where $\mathbf{e}_{jn} = [\mathbf{e}_{jp} \times \mathbf{e}_{js}]$ $(j = 1, 2, 3, 4)$. Vector $\mathbf{e}_{jp}$ is in the incidence plane and is used to set $p$-polarization of $j$-th wave. Vector $\mathbf{e}_{js}$ is perpendicular to incidence plane and is used to set $s$-polarization of $j$-th wave. Vector $\mathbf{e}_{jn}$ matches in direction the wave normal of $j$-th wave. Vector $\mathbf{E}_j$ is a vector of electric field intensity of $j$-th wave and is in the plane containing vectors $\mathbf{e}_{jp}$ and $\mathbf{e}_{js}$. To set orientation of vector $\mathbf{E}_j$ relative to the crystal, polarization azimuth $\psi_j$ is used, which is a measure of angular distance between vectors $\mathbf{e}_{jp}$ and $\mathbf{E}_j$, counted clockwise, when observing along the vector $\mathbf{e}_{jn}$.

The surface of a holographic table is parallel to plane (I), with which the orthonormalized basis $(\mathbf{e}_1, \mathbf{e}_2, \mathbf{e}_3)$ is stiffly joined, where $\mathbf{e}_3 = [\mathbf{e}_1 \times \mathbf{e}_2]$. In fig. 1 vectors $\mathbf{e}_1$ and $\mathbf{e}_3$ lie in plane (I). Coordinate $z$ is counted along the positive direction of axis $Oz$, coinciding in direction with the unit vector $\mathbf{e}_3$. The origin of the $Oz$ axis $(z = 0)$ is taken as the point of its intersection with the face of the crystal (II). The crystal can be rotated around $Oz$ axis, and its position relative to the holographic table is determined using unit vectors $\mathbf{s}$ and $\mathbf{q}$, which are rigidly fixed in the crystallographic coordinate system. Orientation angle $\theta$ is used to give the angle of rotation of the crystal with respect to the axis $Oz$ and is determined as the angular distance between the vectors $\mathbf{e}_2$ and $\mathbf{q}$, which is counted clockwise in the plane (II) from vector $\mathbf{e}_2$ to vector $\mathbf{q}$, when observing toward vector $\mathbf{e}_3$. Let us assume that crystal face (II) and the face parallel thereto are working and covered by an antireflection coating. The distance between these faces is equal to the thickness of $d$ crystal, which is counted from face (II). The angular distance between $\mathbf{e}_{jn}$ vector $\mathbf{e}_{jn}$ and $Oz$ axis is denoted as angle $\varphi_j$, which is counted in the plane of incidence and is equal to the Bragg angle $\varphi_B$.

The insert of fig. 1 shows the orientation of the wave vectors of two transmission $(\mathbf{K}_{13}, \mathbf{K}_{24})$ and four reflective $(\mathbf{K}_{12}, \mathbf{K}_{14}, \mathbf{K}_{23}, \mathbf{K}_{34})$ holographic gratings in the working coordinate system, which can be formed in the opposite four-wave interaction in a photorefractive crystal. Transmission holograms 13 and 24 are formed as a result of pairwise interference, respectively, of pumping wave 1 with signal wave 3 and pumping wave 2 with wave 4. Reflection holographic gratins 14 and 23 are formed by pairwise

interaction of pumping wave 1 with wave 4 and pumping wave 2 with signal wave 3. Interference of pumping waves 1 and 2 causes the formation of a reflection hologram 12. Due to coherent interaction between signal wave 3 and wave 4, a reflection hologram 34 may be formed.

We will search for the stationary solution of the wave equation as a superposition of four linearly polarized light waves:

$$\mathbf{E} = \sum_{j=1}^{4} (E_{jp}\mathbf{e}_{jp} + E_{js}\mathbf{e}_{js}) e^{i\vartheta_j}, \qquad (1)$$

where $\mathbf{E}$ — electric intensity vector of the resultant light field in the crystal, varying along the axis $E_{jp}$, $E_{js}$ — $p$- and $s$-components of vector amplitude $\mathbf{E}_j$, which are functions of coordinate $z$; $\vartheta_j$ — the initial phase of $j$-th wave.

Coherent interaction of light waves produces interference patterns in the crystal. The modulation depth of interference patterns can be found from the following equations:

$$m^{hu} = \left(E_{hs}E_{us} + E_{hp}E_{up}\cos(\mathbf{e}_{hp}\mathbf{e}_{up})\right)/I_0, \qquad (2)$$

where $m^{hu}$ — interference pattern modulation depth $hu$ ($hu = 12,\ 13,\ 14,\ 23,\ 24,\ 34$); $(\mathbf{e}_{hp}\mathbf{e}_{up})$ — scalar vector product. Hereafter, the upper index $hu$ means that the parameter is found with respect to holographic grating $hu$. The resulting intensity of the light field inside the crystal $I_0$ is found by the formula: $I_0 = E_{1s}^2 + E_{1p}^2 + E_{2s}^2 + E_{2p}^2 + E_{3s}^2 + E_{3p}^2 + E_{4s}^2 + E_{4p}^2$.

Using equations (1), (2), the coupled wave equations can be derived from the wave equation in the slowly varying amplitudes approximation, which are further used to analyze the regularities of the contra-directional four-wave mixing on two transmission and four reflection phase-amplitude gratings formed in a photorefractive crystal of $\bar{4}3m$ symmetry class of arbitrary cut:

$$\frac{dE_{1p}}{dz} = (\kappa_{1p2p} + \sigma_{1p2p})E_{2p} + (\kappa_{1p2s} + \sigma_{1p2s})E_{2s} + (\kappa_{1p3p} + \sigma_{1p3p})E_{3p} + (\kappa_{1p3s} + \sigma_{1p3s})E_{3s} + (\kappa_{1p4p} + \sigma_{1p4p})E_{4p} + (\kappa_{1p4s} + \sigma_{1p4s})E_{4s} - \alpha_1 E_{1p}, \qquad (3)$$

$$\frac{dE_{1s}}{dz} = (\kappa_{1s2p} + \sigma_{1s2p})E_{2p} + (\kappa_{1s2s} + \sigma_{1s2s})E_{2s} + (\kappa_{1s3p} + \sigma_{1s3p})E_{3p} + (\kappa_{1s3s} + \sigma_{1s3s})E_{3s} + (\kappa_{1s4p} + \sigma_{1s4p})E_{4p} + (\kappa_{1s4s} + \sigma_{1s4s})E_{4s} - \alpha_1 E_{1s}, \qquad (4)$$

$$\frac{dE_{2p}}{dz} = (-\kappa_{2p1p} + \sigma_{2p1p})E_{1p} + (-\kappa_{2p1s} + \sigma_{2p1s})E_{1s} + (\kappa_{2p3p} + \sigma_{2p3p})E_{3p} + (\kappa_{2p3s} + \sigma_{2p3s})E_{3s} + (\kappa_{2p4p} + \sigma_{2p4p})E_{4p} + (\kappa_{2p4s} + \sigma_{2p4s})E_{4s} - \alpha_2 E_{2p}, \qquad (5)$$

$$\frac{dE_{2s}}{dz} = (-\kappa_{2s1p} + \sigma_{2s1p})E_{1p} + (-\kappa_{2s1s} + \sigma_{2s1s})E_{1s} + (\kappa_{2s3p} + \sigma_{2s3p})E_{3p} + (\kappa_{2s3s} + \sigma_{2s3s})E_{3s} + (\kappa_{2s4p} + \sigma_{2s4p})E_{4p} + (\kappa_{2s4s} + \sigma_{2s4s})E_{4s} - \alpha_2 E_{2s}, \qquad (6)$$

$$\frac{dE_{3p}}{dz} = (-\kappa_{3p1p} + \sigma_{3p1p})E_{1p} + (-\kappa_{3p1s} + \sigma_{3p1s})E_{1s} + (-\kappa_{3p2p} + \sigma_{3p2p})E_{2p} + (-\kappa_{3p2s} + \sigma_{3p2s})E_{2s} + (\kappa_{3p4p} + \sigma_{3p4p})E_{4p} + (\kappa_{3p4s} + \sigma_{3p4s})E_{4s} - \alpha_3 E_{3p}, \qquad (7)$$

$$\frac{dE_{3s}}{dz} = (-\kappa_{3s1p} + \sigma_{3s1p})E_{1p} + (-\kappa_{3s1s} + \sigma_{3s1s})E_{1s} + (-\kappa_{3s2p} + \sigma_{3s2p})E_{2p} + (-\kappa_{3s2s} + \sigma_{3s2s})E_{2s} + (\kappa_{3s4p} + \sigma_{3s4p})E_{4p} + (\kappa_{3s4s} + \sigma_{3s4s})E_{4s} - \alpha_3 E_{3s}, \qquad (8)$$

$$\frac{dE_{4p}}{dz} = (-\kappa_{4p1p} + \sigma_{4p1p})E_{1p} + (-\kappa_{4p1s} + \sigma_{4p1s})E_{1s} + (-\kappa_{4p2p} + \sigma_{4p2p})E_{2p} + (-\kappa_{4p2s} + \sigma_{4p2s})E_{2s} + (-\kappa_{4p3p} + \sigma_{4p3p})E_{3p} + (-\kappa_{4p3s} + \sigma_{4p3s})E_{3s} - \alpha_4 E_{4p}, \qquad (9)$$

$$\frac{dE_{4s}}{dz} = (-\kappa_{4s1p} + \sigma_{4s1p})E_{1p} + (-\kappa_{4s1s} + \sigma_{4s1s})E_{1s} + (-\kappa_{4s2p} + \sigma_{4s2p})E_{2p} + (-\kappa_{4s2s} + \sigma_{4s2s})E_{2s} + (-\kappa_{4s3p} + \sigma_{4s3p})E_{3p} + (-\kappa_{4s3s} + \sigma_{4s3s})E_{3s} - \alpha_4 E_{4s}. \qquad (10)$$

In coupled wave equations the following notations are agreed: $\kappa_{hbut} = \left(\kappa_0(\mathbf{e}_{hb}\Delta\hat{\eta}^{hu}\mathbf{e}_{ut})\right)/\cos\varphi_h$, $\sigma_{hbut} = \left(\sigma_0(\mathbf{e}_{hb}\Delta\hat{\sigma}^{hu}\mathbf{e}_{ut})\right)/\cos\varphi_h$, $\alpha_h = \alpha/\cos\varphi_h$, where $\kappa_0 = \pi n_0^3/(2\lambda)$ — coupling constant of phase holographic grating, $\sigma_0 = -\pi/(nc)$ — coupling constant of amplitude holographic grating, $\Delta\hat{\eta}^{hu}$ — disturbances of inverse tensor of dielectric permeability of crystal, compliant with phase holographic grating $hu$, $\Delta\hat{\sigma}^{hu}$ — disturbances of crystal conductivity tensor, compliant with amplitude holographic grating $hu$, $n_0$ — refraction index of undisturbed crystal, $\alpha$ — coefficient of natural absorption of crystal, $\lambda$ — wave length, $c$ — speed of light in vacuum; $h,\ u = 1, 2, 3, 4$; $b,\ t = p,\ s$. Equations to find disturbances of the inverse dielectric permeability tensor $\Delta\hat{\eta}^{hu}$ of a cubic crystal taking into account the joint action of photoelastic and inverse piezoelectric effects are given in [23]. Disturbances of cubic crystal conductivity tensor in the linear approximation by contrast are calculated from the following equation: $\Delta\hat{\sigma}^{hu} = m^{hu}\sigma^{hu}\delta_{kn}$, where $\sigma^{hu}$ — conductivity coefficients, $\delta_{kn}$ — single symmetric second rank tensor. To derive the coupled wave equations (3)–(10), it was assumed that the spatial shifts of the phase and amplitude gratings with respect to the corresponding interference patterns are $\pi/2$ and 0, respectively.

When solving the coupled wave equations (3)–(10), parameters of GaAs crystal were used, compliant with wave length $\lambda = 1064 \cdot 10^{-9}$ m and borrowed from papers [19,24,25]: absorption index $\alpha = 410\,\mathrm{m}^{-1}$ [19]; refraction index of undisturbed crystal $n_0 = 3.48$ [24]; electrooptic coefficient $r_{41} = -1.43 \cdot 10^{-12}$ m/V [24]; elasticity coefficients $c_1 = 11.88 \cdot 10^{10}\,\mathrm{N/m^2}$, $c_2 = 5.38 \cdot 10^{10}\,\mathrm{N/m^2}$, $c_3 = 5.94 \cdot 10^{10}\,\mathrm{N/m^2}$ [24]; photoelastic effect coefficients $p_1 = -0.165$, $p_2 = p_3 = -0.14$, $p_4 = -0.072$ [25]; piezoelectric coefficient $e_{14} = 0.154\,\mathrm{C/m^2}$ [24]. Here we adopt

the following notations for the nonzero components of the linear electrooptic ($\hat{r}^S$), photoelastic ($\hat{p}^E$) and inverse piezoelectric ($\hat{e}$) effects and elasticity tensor ($\hat{c}^E$) components: $r^S_{123} = r^S_{132} = r^S_{213} = r^S_{231} = r^S_{312} = r^S_{321} \equiv r_{41}$, $p^E_{11} = p^E_{22} = p^E_{33} \equiv p_1$, $p^E_{12} = p^E_{23} = p^E_{31} \equiv p_2$, $p^E_{13} = p^E_{21} = p^E_{32} \equiv p_3$, $p^E_{44} = p^E_{55} = p^E_{66} \equiv p_4$, $e_{123} = e_{132} = e_{123} = e_{231} = e_{312} = e_{321} \equiv e_{14}$, $c^E_{11} = c^E_{22} = c^E_{33} \equiv c_1$, $c^E_{12} = c^E_{13} = c^E_{23} = c^E_{21} = c^E_{31} = c^E_{32} \equiv c_2$, $c^E_{44} = c^E_{55} = c^E_{66} \equiv c_3$.

The index $S$ for the linear electrooptic effect tensor $\hat{r}^S$ means that the $r_{41}$ component of the linear electrooptic effect tensor was measured for the clamped crystal; the components of the elasticity $\hat{c}^E$ and photoelastic effect $\hat{p}^E$ tensors were measured at a constant electric field. In the calculations, the ratios of light wave intensities and the value of the Bragg angle $\varphi_B$ in air were chosen based on the data presented in [19]. Initial conditions for solving the two-point boundary problem were chosen as follows: $E_{1p}(0) = E_1 \cos\psi_1$, $E_{1s}(0) = E_1 \sin\psi_1$, $E_{2p}(d) = E_2 \cos\psi_2$, $E_{2s}(d) = E_2 \sin\psi_2$, $E_{3p}(0) = E_3 \cos\psi_3$, $E_{3s}(0) = E_3 \sin\psi_3$, $E_{4p}(d) = 0$, $E_{4s}(d) = 0$.

The numerical solution of the coupled wave equations (3)–(10) was performed using the well-known shooting method [26].

## Produced findings and their analysis

Fig. 2 and 3 present curves of dependencies of p-polarized ($I_{4p}$ in fig. 2, *a* and fig. 3, *b*) and s-polarized ($I_{4s}$ in fig. 2, *b* and fig. 3, *a*) components of wave 4 from orientation angle $\theta$, which are produced by theoretical and experimental methods when researching the contra-directional four-wave mixing in GaAs crystal of (110)-cut with thickness of $d = 1.5 \cdot 10^{-3}$ m. Data in fig. 2 and 3 is produced for cases when pumping wave 1 and signal wave 3 have the same *s*-polarization, and pumping wave 2 is polarized either in incidence plane (fig. 2), or perpendicularly thereto (fig. 3). Dark points in figures correspond to experimental data given in [19] and indicate orientation dependencies $I_{4p}(\theta)$ and $I_{4s}(\theta)$. Dashed lines in fig. 2 and 3 correspond to curves of dependencies $I_{4p}(\theta)$ and $I_{4s}(\theta)$, produced in [19] based on analytical solution of coupled waves equations.

As seen from the figures, periodicities of $I_{4p}(\theta)$ and $I_{4s}(\theta)$ dependence curves produced by theoretical and experimental method are practically the same. Whereas when comparing theoretically calculated curve of dependence with the corresponding experimental curve it may be detected that in the surroundings of local maxima the intensity values $I_{4p}$ ($I_{4s}$), produced theoretically and experimentally, may differ significantly. For example, if *p*-polarized pumping wave 2 is used, theoretically calculated value $I_{4p}$ in the local maximum of dependence $I_{4p}(\theta)$ (fig. 2, *a*), achieved at $\theta \approx 320°$, exceeds experimental value $I_{4p}$ practically twice. A similar difference between the intensity values $I_{4s}$ obtained theoretically and experimentally at *p*-polarized pumping wave 2, is

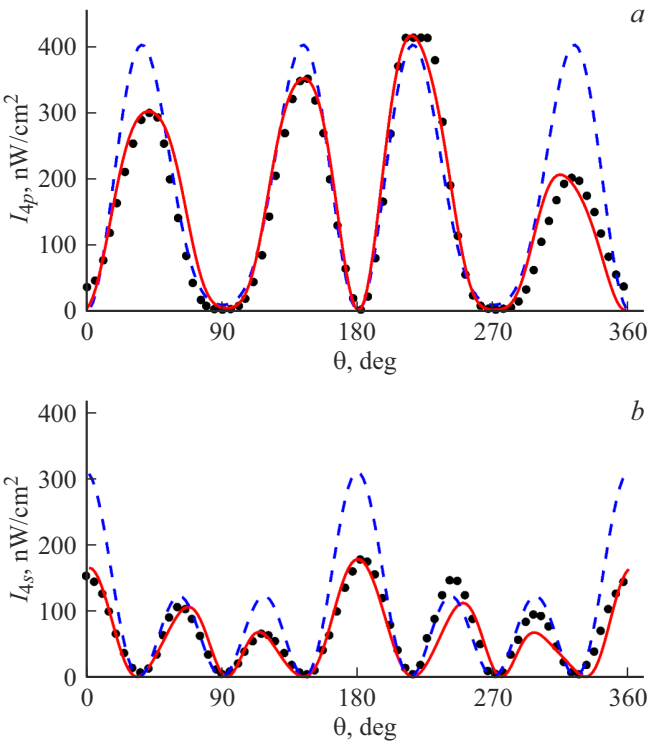


**Figure 2.** Dependencies of intensities of *p*-polarized (*a*) and *s*-polarized (*b*) components of light wave 4 from oriented angle $\theta$ at *p*-polarized wave 2: points — experiment given in paper [19]; dashed line — theoretical curve given in [19]; solid line — theoretical curve produced on the basis of numerical solution of coupled waves equations (3)–(10).

achieved at the local maximum of the dependence graph $I_{4s}(\theta)$, corresponding to the zero value of the orientation angle (fig. 2, *b*). When *s*-polarized pumping wave 2 is used, the largest difference between the intensities of the wave 4 components determined theoretically and experimentally is noticeably smaller. When intensity of *s*-polarized component of wave 4 was found in case when pumping wave 2 has *s*-polarization, the largest difference is obtained at $\theta \approx 270°$ (fig. 3, *a*): experimentally found value $I_{4s}$ is higher than the theoretically calculated one approximately 1.45 times. The largest difference in local maxima of graphs $I_{4p}(\theta)$, obtained theoretically and experimentally, in case of *s*-polarized pumping wave 2 is achieved at $\theta \approx 0°$. In this case, the theoretically calculated value of $I_{4p}$ is 1.7 times greater than the experimental value.

If we consider the theoretical graphs of the dependence $I_{4p}(\theta)$ and $I_{4s}(\theta)$ obtained in [19], we can see that the intensity values in the local maxima are either equal to each other, or correspond to two different values. For example, in fig. 2, *a* values $I_{4p}$ in the local maxima of the dependence graph $I_{4p}(\theta)$ are almost equal and approximately equal amount to 400 nW/cm$^2$. In fig. 2, *b* and fig. 3 the values of intensities in the local maxima of dependence graphs $I_{4p}(\theta)$ and $I_{4s}(\theta)$ are equal to

300 nW/cm$^2$ or 120 nW/cm$^2$. However, this does not quite correspond to the experimental data given in [19]. As can be seen from figs. 2 and 3, the values of $I_{4p}$ and $I_{4s}$ in the local maxima of the experimental curves do not correspond to one or two fixed values and can differ significantly from each other. Such a difference in the theoretical and experimental data may be caused by neglecting a number of properties of the crystalline medium and the holographic gratings formed in the photorefractive semiconductor in the theoretical model. It is stated in [19] that the difference in the theoretical and experimental data may be due to the lack of accounting for diffraction contribution of light waves on the amplitude holographic gratings formed in a GaAs crystal. At the same time it should be noted that the possibility of simultaneous recording of several holographic gratings in the contra-directional four-wave mixing in a photorefractive crystal was not taken into account in this paper. Besides, influence of photoelastic and inverse piezoelectric effects, which may have a significant effect on the polarization and energy characteristics of the light beams diffracted on the holographic gratings [27], was neglected in the coupled wave equations given in [19].

In Figs. 2 and 3 the dependence graphs $I_{4p}(\theta)$ and $I_{4s}(\theta)$ are shown in solid lines, which are obtained from the numerical solution of the coupled wave equations (3)–(10). A number of assumptions were made when calculating the theoretical curves. It was assumed that the four-wave interaction produced 2 transmission and 4 reflection holographic gratings. It was assumed that the transmission holographic gratings, which correspond to wave vectors $\mathbf{K}_{13}$ and $\mathbf{K}_{24}$, and the reflection holographic gratings, which correspond to wave vectors $\mathbf{K}_{12}$ and $\mathbf{K}_{34}$, have a phase-amplitude structure. When pumping wave 2 interacts with signal wave 3 and pumping wave 1 - with wave 4, reflection holographic gratings with wave vectors directed parallel to the crystallographic direction [110] are formed. In this case, phase reflection holographic gratings in cubic photorefractive crystals are not formed [28], and to solve the coupled wave equations (3)–(10) it was assumed that the reflection gratings are purely amplitude. The calculations also took into account the joint contribution of photoelastic and inverse piezoelectric effects in the formation of the holographic gratings, as well as the absorption of the GaAs crystal.

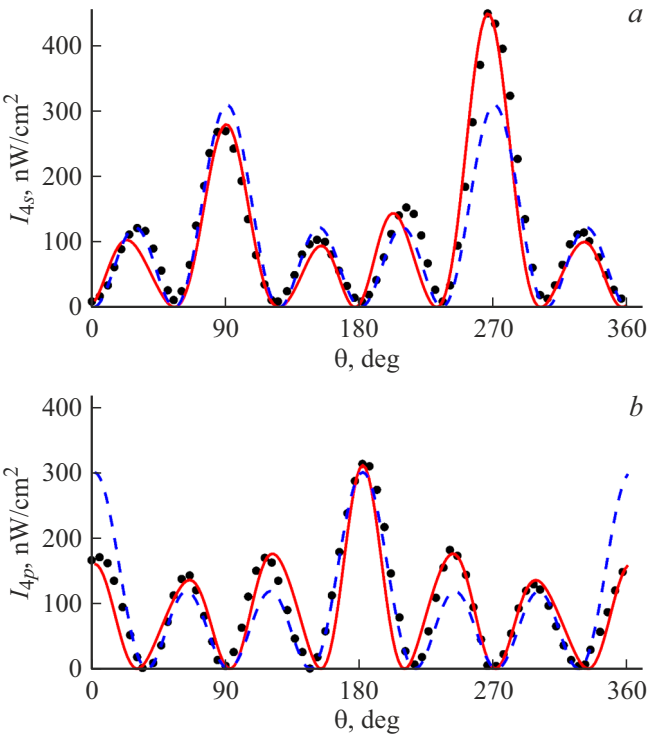


**Figure 3.** Dependencies of intensities of $s$-polarized ($a$) and $p$-polarized ($b$) components of light wave 4 from oriented angle $\theta$ at $s$-polarized wave 2: points — experiment given in paper [19]; dashed line — theoretical curve given in [19]; solid line — theoretical curve produced on the basis of numerical solution of coupled waves equations (3)–(10).

As follows from figs. 2 and 3, in the numerical calculations the joint account of the above factors makes it possible not only to achieve a coincidence of the periodicity of the theoretical and experimental curves, but also to reach coordination of the intensities in the polarization components of wave 4 in the surroundings of the local maxima in the dependence graphs $I_{4p}(\theta)$ and $I_{4s}(\theta)$. For example, if to obtain the coupled wave equations (3)–(10), diffraction of light waves is taken into account simultaneously on several holographic gratings, it leads to difference of intensity values in the local maxima of the dependence graphs $I_{4p}(\theta)$ and $I_{4s}(\theta)$. Appropriate selection of electric field intensity values for the spatial charge in the photorefractive semiconductor and the amplitude coupling constants can achieve a more accurate coincidence between the theoretical and experimental data. Results of numerical simulation show that changing phase and amplitude coupling constants of one of six holographic gratings does not necessarily lead to intensity changes simultaneously in all local maxima of the dependence graph. As a rule, varying the phase and amplitude coupling constants of the holographic grating leads to changing the values $I_{4p}$ and $I_{4s}$ in the local maxima, symmetrically located relative to the values of orientation angles.

Consideration of the joint contribution of the photoelastic and inverse piezoelectric effects in the guided wave equations influences significantly the dependence graphs $I_{4p}(\theta)$, $I_{4s}(\theta)$ and is one of the conditions for the successful coordination of the theoretical and experimental curves. Under the influence of these effects, depending on the orientation angle, there may be both an increase in the intensity of the polarization component of the wave 4 and its decrease. In this case there is a small (about several degrees) change in the values of the orientation angle, when local maxima of dependence graphs $I_{4p}(\theta)$ and $I_{4s}(\theta)$ are reached. When „is included“ in the guided wave equations (3)–(10)

of crystal absorption, there is a quantitative decrease in the intensity of the polarization component of wave 4. The greatest decrease in intensity is achieved in the surroundings of the local maxima of $I_{4p}(\theta)$ and $I_{4s}(\theta)$ dependence graphs. In the surroundings of local maxima the intensity remains practically unchanged. No qualitative transformation of $I_{4p}(\theta)$ and $I_{4s}(\theta)$ dependence graphs has been observed during „inclusion of" crystal absorption.

## Conclusion

A system of guided wave equations suitable for calculating degenerate contra-directional four-wave mixing on 6 holographic (2 transmission and 4 reflection) phase-amplitude holographic gratings formed in a cubic photorefractive crystal of 43*m* symmetry class is presented. When the mathematical model was constructed, the case was considered when the light waves incident on the crystal have linear polarization, and the crystal grating has an arbitrary orientation relative to the holographic table. The joint contribution of linear electro-optical, photoelastic, and inverse piezoelectric effects has been taken into account in the mathematical model, as well as crystal absorption.

Based on comparison of the results of the numerical solution of the obtained guided wave equations with the known experimental data, it is shown that more accurate results of calculating the intensity of the polarization components of the reversed wave are achieved when the contributions of all diffraction processes occurring on the transmission and reflection holographic gratings formed during opposite four-wave interaction in the photorefractive crystal are promptly taken into account. At the same time it should be noted that a photorefractive semiconductor may form holographic gratings with phase-amplitude structure. Accounting of the photoelastic effect together with the inverse piezoelectric effect and crystal absorption leads to a more accurate prediction of the local maxima in graphs of dependences between reverse wave polarization component intensity and orientation angle.

### Funding

The paper was prepared with the financial support of the Ministry of Education of the Republic of Belarus (agreement dated March 22, 2021 № 1410/2021) within the State Program of Scientific Research № 6 „Photonics and electronics for innovations" for 2021–2025 . (assignment 6.1.14).

## References

[1] V.M. Petrov, A.V. Shamray. *Interferentsiya i diffraktsiya dlya interferentsionnoy fotoniki* (Lan, SPb., 2019) (in Russian).
[2] S.G. Odulov, M.S. Soskin, A.I. Khizhnyak. *Lazery na dinamicheskikh reshetkakh: opticheskie generatory na chetyrekhvolnovom smeshenii* (Nauka, M. 1990) (in Russian).
[3] M.P. Petrov, S.I. Stepanov, A.V. Khomenko. *Fotoreaktivnye kristally v kogerentnoy optike* (Nauka, SPb, 1992) (in Russian).
[4] M.B. Klein. Opt. Lett. **9** (8), 350 (1984).
[5] A.M. Glass, A.M. Johnson, D.H. Olson, W. Simpson, A.A. Ballman. Appl. Phys. Lett. **44** (10), 948 (1984).
[6] M.B. Klein, S.W. Mc Cahon, T.F. Boggess, G.C. Valley. J. Opt. Soc. Am. B. **5** (12), 2467 (1988).
[7] H. Rajbenbach, B. Imbert, J.P. Huignard, S. Mallick. Opt. Lett. **14** (1), 78 (1989).
[8] G. Gheen, L.-J. Cheng. Appl. Phys. Lett. **51** (19), 1481 (1987).
[9] R. Nietzke, P.Panknin, W. Elsässer, E.O. Göbel IEEE J. Quant. Electron. **25** (6), 1399 (1989).
[10] T. Sadeev, H. Huang, D. Arsenijevic, K. Schires, F. Grillot, D. Bimberg. Appl. Phys. Lett. **107**, 191111 (2015).
[11] I.A. Solovev, Yu.V. Kapitonov, B.V. Stroganov, Yu.P. Efimov, S.A. Eliseev, S.V. Poltavtsev. J. Physics: Conf. Series. **1124**, 051042 (2018).
[12] K. Je, K. Kyhm. Rapid Res. Lett. 1800354 (2018).
[13] A.A. Izvanov, A.E. Mandel, N.D. Khatkov, S.M. Shandarov. Avtometriya. **2**, 79 (1986) (in Russian).
[14] S.I. Stepanov, S.M. Shandarov, N.D. Khatkov. FTT. **29** (10), 3054 (1987) (in Russian).
[15] H. Kogelnik. Bell Syst. Tech. J. **48**, 2909 (1969).
[16] G. Montemezzani, M. Zgonik. Phys. Rev. E. **55** (1), 1035 (1997).
[17] V.V. Shepelevich, A.V. Makarevich, S.M. Shandarov. Tech. Phys. Lett. **40** (11), 1024 (2014).
[18] R.B. Bylsma, D.H. Olson, A.M. Glass. Opt. Lett. **13** (10), 853 (1988).
[19] Y. Ding, H.J. Eichler. Opt. Comm. **110**, 456 (1994).
[20] R.V. Litvinov, S.I. Polkovnikov, S.M. Shandarov. Quant. Electron. **31** (2), 167 (2001).
[21] A.V. Gusel'nikova, S.M. Shandarov, A.M. Plesovskikh, R.V. Romashko, Yu.N. Kulchin. J. Opt. Technol. **73** (11), 760 (2006).
[22] V.N. Naunyka, S.F. Nichiporko, A.V. Makarevich, S.M. Shandarov. Tech. Phys. **66** (5), 808 (2021).
[23] S.M. Shandarov, V.V. Shepelevich, N.D. Khatkov. Opt. Spectrosc. **70** (5), 627 (1991).
[24] K. Shcherbin, S. Odoulov, R. Litvinov, E. Shandarov, S. Shandarov. J. Opt. Soc. Am. B. **13** (10), 2268 (1996).
[25] A. Dargys, J. Kundrotas. *Handbook on physical properties of Ge, Si, GaAs and InP* (Science and Encyclopedia Publishers, 1994).
[26] Y.H. Ja. Opt. and Quant. Electron. **15**, 539 (1983).
[27] V.V. Shepelevich, N.N. Egorov, V. Shepelevich. J. Opt. Soc. Am. B. **11** (8), 1394 (1994).
[28] V.V. Shepelevich, V.N. Naunyka. J. Holography Speckle. **5** (3), 286 (2009).